Thermal and Optical Characterization of Photonic Integrated Circuits by Thermoreflectance Microscopy

Joseph A. Summers, *Member, IEEE*, Maryam Farzaneh, Rajeev J. Ram, *Senior Member, IEEE*, and Janice A. Hudgings, *Senior Member, IEEE*

***Abstract*—We report high resolution, non-invasive, thermal and optical characterization of semiconductor optical amplifiers (SOAs) and SOA-based photonic integrated circuits (PICs) using thermoreflectance microscopy. Chip-scale temperature imaging of SOAs and PICs, along with an energy balance model, are used to calculate the optical power distribution within and between SOAs to determine optical gain, fiber coupling loss, and passive component loss under normal device operating conditions. This technique is demonstrated to map optical power in SOA-based Mach–Zehnder interferometer (SOA-MZI) PICs, with close agreement with photocurrent and fiber-coupled measurements. The use of amplified spontaneous emission (ASE) for fiber-free characterization of the PICs is also shown, enabling non-invasive, wafer-scale testing prior to packaging.**

***Index Terms*—Integrated optoelectronics, semiconductor optical amplifiers, temperature, temperature measurement.**

I. Introduction

PHOTONIC integrated circuits (PICs) have the promise of reducing the manufacturing and packaging costs of complex optical systems via miniaturization and monolithic integration of multiple optoelectronic devices on a single chip. PICs are usually comprised of active optoelectronic devices, such as lasers and semiconductor optical amplifiers (SOAs), that are integrated on-chip with passive components, such as couplers, filters, and routers. Integration of active and passive components is typically accomplished using a monolithic fabrication process, after which the chip is fiber-coupled to provide the necessary optical inputs and outputs [1]. PICs have growing applications in optical fiber communication [2], where SOA-based PICs have been demonstrated as all-optical logic gates, switches [3], and wavelength converters for photonic regeneration, wavelength routing, and switching [4]–[6].

Monolithic integration of optoelectronic devices into PICs restricts direct access and measurement of the input and output optical signals of individual components after fabrication, which makes it difficult to precisely measure optical power within and between integrated devices. In addition, as the number and density of devices on a single chip grows, heat dissipation and thermal effects, such as thermal cross-talk and SOA gain reduction, become increasingly important issues that can adversely affect the performance of the PIC. Techniques such as spontaneous emission spectroscopy [7] and split-contact voltage profiling [8] have been employed to study the optical performance of stand-alone SOAs without direct access to the optical input and output. However, these methods require structural modification of the SOAs and hence are of limited use in characterization of standard PICs. On-chip electrical measurements such as IV curves [9] and photocurrent measurements [10] are additional methods that can be used, respectively, to identify catastrophic failures, or to estimate optical power absorbed by an SOA from a coupled fiber or integrated waveguide. However, these techniques provide little information about active material parameters under normal PIC operating conditions, and they give no information about the spatial distribution of optical power within each active device.

Prior work has demonstrated that spatial profiling of the surface temperature of individual active optoelectronic devices using micro-thermocouples can be used to determine the internal optical power distribution and to characterize optical properties such as gain, quantum efficiency, and saturation power of these devices, without direct optical measurements [11], [12]. However, this method suffers from a low spatial resolution due to the size of the thermocouple wires and is impractical for use on an integrated chip comprised of multiple devices.

In this work, we use a non-contact, high resolution, two-dimensional thermoreflectance imaging technique, in combination with a heat exchange model, to demonstrate the application of chip-scale temperature profiling for thermal and optical characterization of stand-alone SOAs and PICs. Thermal imaging is used as a diagnostic tool for failure analysis, thermal management, and for characterizing the optical performance of component devices under operating conditions. We show quantitative measurement of fiber coupling loss, amplification in each SOA, and passive loss between SOAs, as a means to map the optical power distribution throughout the PIC. In addition, we demonstrate the application of the thermal imaging technique for fiber-free testing of PICs by using amplified spontaneous emission (ASE) from an on-chip SOA instead of the usual external optical source. This method can be used at the wafer level, before packaging and fiber-coupling, both to diagnose catastrophic failures as a complementary method to photocurrent

Manuscript received February 26, 2009; revised April 10, 2009. Current version published December 03, 2009. This work was supported by the National Science Foundation, under Grant ECS-0134228 and Grant DMI-0531171, the Photonics Technology Access Program, and the Research Corporation.

M. Farzeneh was with the Department of Physics, Mount Holyoke College, South Hadley, MA 01075 USA, and is now with the Department of Physics and Astronomy, Denison University, Granville, OH 43023 USA (e-mail: farzanehm@denison.edu).

J. A. Summers and J. A. Hudgings are with the Department of Physics, Mount Holyoke College, South Hadley, MA 01075 USA (e-mail: jsummers@mtholyoke.edu; jhudging@mtholyoke.edu).

R. J. Ram is with the Research Laboratory of Electronics, Massachusetts Institute of Technology, Cambridge, MA 02139 USA (e-mail: rajeev@mit.edu).

Digital Object Identifier 10.1109/JQE.2009.2022648

measurements, and also for extraction of material parameters such as modal gain, which cannot be obtained by conventional electronic methods [13].

Such information obtained from thermoreflectance measurements of PICs would be valuable for improvements in chip thermal management, design of individual devices and the PIC layout, and reduction of manufacturing costs.

II. Experimental Procedure

The integrated PICs, provided by Alphion Corporation, are two fiber-coupled chips comprised of active SOA elements interconnected in multiple stages by passive optical waveguides, s-bends, and multimode interference (MMI) splitters, with a typical operating wavelength of 1550 nm. The first PIC consists of 10 SOAs and 6 MMIs that form nested SOA-based Mach–Zehnder interferometer (MZI) structures with input and output amplifiers. The second device, used in the fiber-free characterization experiments, has 6 SOAs and 5 MMIs. All the cascaded SOAs are overlaid with gold electrical contacts. Both chips are based on a proprietary monolithic active-passive InP integration platform and are enclosed in a 24-pin butterfly package which includes a thermistor and a thermoelectric cooler to provide a stable and controlled operating temperature [14].

Throughout this work, thermoreflectance imaging is used to measure the temperature distribution of the gold electrical contacts along the top of the 2 μm-wide waveguide of the individual and integrated SOAs. Thermoreflectance microscopy measures the normalized change in surface reflectivity $(\Delta R/R)$ due to modulation of surface temperature (ΔT)

$$\frac{\Delta R}{R} = \left(\frac{1}{R}\frac{\partial R}{\partial T}\right)\Delta T \equiv \kappa \Delta T \tag{1}$$

where κ is the thermoreflectance calibration coefficient, which depends on the material and illumination wavelength [15]. It is good practice to determine the value of κ experimentally through a calibration procedure, since changes in material composition, layer thickness, or surface roughness may change its effective value. In this work, thermoreflectance measurements are performed using an experimental setup similar to that of [16] with a $5\times$, NA $= 0.1$ microscope objective and a blue $(\lambda = 467$ nm$)$ light-emitting diode (LED) as the illumination source, resulting in 2 μm spatial resolution. Using a 12-bit, 60 Hz charge-coupled device (CCD) camera as a detector enables two dimensional thermal imaging. A Chroma BG-39 short-pass filter placed in front of the CCD attenuates any emission from SOAs and the 1550 nm distributed feedback (DFB) laser used to optically inject the SOAs, nominally better than 10^{-15} while transmitting around 85% of the blue thermoreflectance illumination reflected from the chip. Using micro-thermocouples, a value of $\kappa \approx 5 \times 10^{-4}$ K^{-1} for the thermoreflectance calibration coefficient of the gold contact layers is measured. This value of κ differs slightly from our previously reported results $(\kappa \approx 3.29 \times 10^{-4})$ [13], and the data presented in Section IV-C has been rescaled to incorporate this change in κ. In all the experiments involving the integrated devices, the heat sink temperature is actively controlled at 25°C.

The thermoreflectance measurements are acquired using the "four bucket" technique, in which the CCD camera is phase locked to the modulation frequency f of the temperature of the test device, and is triggered at frequency $4f$. Real-time signal processing of the four images per period effectively performs pixel-by-pixel lock-in amplification on the resulting surface reflectivity signal [17]. The required temperature modulation ΔT in the SOAs is achieved by one of two methods, depending on the physical characteristic of interest. Modulating the SOA bias current at a frequency f with no external light injection causes the thermoreflectance apparatus to "lock-in" on the electrical heating of the surface of the test device. Alternatively, in order to investigate radiative optical cooling during amplification (or heating from optical absorption), the temperature modulation ΔT can be obtained by applying a DC electrical bias to the SOA while modulating the input optical signal at frequency f, phase locked to the fourth sub-harmonic of the CCD camera trigger.

III. Energy Balance Model: Extracting Optical Characteristics From Thermal Distribution

In prior work, we have shown that detailed surface thermal profiling, in combination with a total energy balance model, can be used to extract the internal optical power distribution in an operating SOA [11], [12], [18]. For example, under normal biasing conditions, amplification of an injected optical signal causes the SOA's surface temperature to decrease exponentially along its length, due to radiative cooling by the emitted photons [12]. Alternatively, when unbiased, an SOA behaves as an optical absorber. In this case, the net absorption of injected photons results in heating which mostly occurs near the SOA input, with a decaying profile along the device length [11].

Building on this prior work, a finite element energy balance model is used to describe the heat exchange mechanisms and thermal profile of the individual devices under test [18]. Fig. 1 shows a schematic of an SOA under normal operating conditions. For a differential element of length δx at position x_i along the length of an amplifier or absorber, the model can be written as

$$P_{el}\frac{\delta x}{L} = \frac{dP_{rad}(x_i)}{dx}\delta x + \left[\frac{T_s(x_i) - T_{hs}}{Z_T}\right]\frac{\delta x}{L} + \left[A_{\text{eff}} \cdot h\left(T_s(x_i) - T_a\right)\right]\frac{\delta x}{L} \tag{2}$$

where L is the length of the device, $P_{el} = \text{IV}$ is the electrical power, and $P_{rad} = P_{\text{out}} - P_{\text{in}}$ is the radiated optical power defined as the difference between the output and input optical powers. P_{rad} is positive for an amplifier and negative for an absorber.

The second term on the right-hand side of (2) represents vertical heat conduction between the device surface at temperature T_s and the heat sink at temperature T_{hs} with effective vertical thermal impedance Z_T. Convection from the surface plane with effective area A_{eff} and convection coefficient h is described by the third term on the right, where the ambient temperature T_a is taken to be a constant. Since lateral thermal impedance is considerably larger than Z_T [11], [12], the effects of lateral heat conduction are neglected.

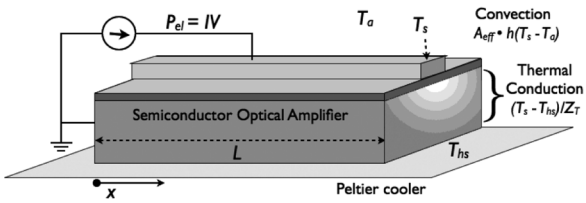

Fig. 1. Schematic of an SOA under normal operating conditions, where P_{el} represents electrical power injected into the device, Z_T represents the thermal impedance from the active region to the substrate, and $A_{\text{eff}} \bullet h$ represents convective cooling from the surface.

Thermoreflectance imaging enables us to determine the modulation of the surface temperature ΔT_s as a result of modulating either the electrical power by ΔP_{el}, or the radiated optical power by ΔP_{rad}, at frequency f. The change in the heat sink temperature can be taken to be proportional to the surface temperature change ($\Delta T_{hs} = \gamma \Delta T_s$), which has been experimentally verified. Incorporating the relevant modulations, the energy balance model in its general form, after integration over the length of the device, can be written as

$$\Delta P_{el} = \Delta P_{rad}^{(t)} + \frac{c}{L}\int_0^L \Delta T_s(x)dx \tag{3}$$

where $\Delta P_{rad}^{(t)} = \Delta P_{\text{out}} - \Delta P_{\text{in}}$ is the total modulated change in radiated optical power along the device length. $c = A_{\text{eff}} \cdot h + (1-\gamma)/Z_T$ is a constant relating material-dependent convection and conduction properties; this constant is experimentally quantified below.

In the case of electrical heating with no optical injection, since the radiated power from amplified spontaneous emission (ASE) is small and negligible, the total radiated power $\Delta P_{rad}^{(t)} \approx 0$, and

$$\Delta P_{el} = \frac{c}{L}\int_0^L \Delta T_s^{(el)}(x)dx. \tag{4}$$

Here, $\Delta T_s^{(el)}(x) > 0$ is the change in surface temperature of the device at position x along its length due to electrical heating.

In the second modulation scenario, in which the electrical bias is fixed, $\Delta P_{el} \approx 0$, and the optical input power is modulated, (3) reduces to

$$\Delta P_{rad}^{(t)} = \Delta P_{\text{out}} - \Delta P_{\text{in}} = -\frac{c}{L}\int_0^L \Delta T_s^{(opt)}(x)dx. \tag{5}$$

In the case of an operating SOA, $\Delta T_s^{(opt)}(x) < 0$ is the local decrease in surface temperature due to amplification of the modulated optical signal. Similarly, if the SOA is kept unbiased under optical injection, it acts as an absorber with $\Delta T_s^{(opt)}(x) > 0$, resulting in a negative $\Delta P_{rad}^{(t)}$.

This model is generally valid for a variety of SOA materials and layer structures, assuming that the vast majority of heating and cooling occur in the active heterostructure region of the device [18]. This assumption will be valid for most SOAs, and the lumped thermal parameters can be easily extracted using a calibration technique that is described in Section IV.

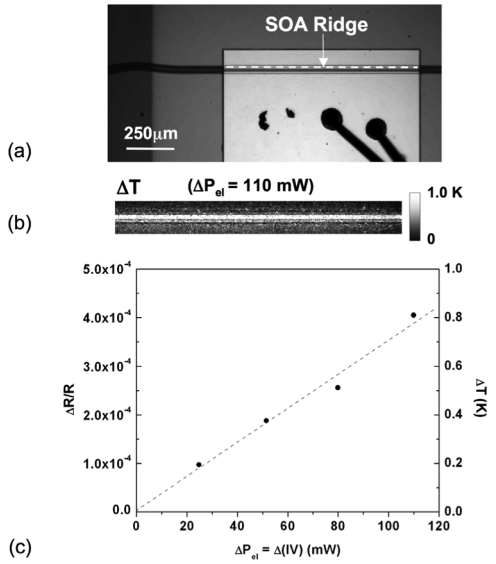

Fig. 2. Electrical heating in an SOA. (a) A micrograph of the SOA. (b) Thermal image measured by thermoreflectance due to electrical heating. (c) Temperature (ΔT) versus electrical power (ΔP_{el}) measurements used to extract c/L. The SOA ridge data are the average temperatures measured at the top of the 2 μm-wide waveguide along the entire length of the SOA.

IV. Results and Discussion

In this section we show the application of the thermal imaging technique along with the energy balance model of Section III for thermal and optical characterization of individual SOAs [19], as well as cascaded devices where direct access to optical signals is limited.

A. Electrical Pumping of an SOA for Thermal Imaging and Extraction of c/L Parameter

Fig. 2(a) shows a micrograph of SOA 1 from the Alphion PIC [schematic, Fig. 4(b)], under 5 × magnification. The change in surface temperature of the SOA due to electrical heating, as measured by thermoreflectance microscopy, is shown in the thermal image in Fig. 2(b). The bias current of the SOA is modulated with a square wave at $f = 15$ Hz around a dc value of $I_0 = 90$ mA, with a peak-to-peak current swing $\Delta I = 80$ mA ($\Delta P_{el} = 110$ mW). For 5 × magnification, the spatial resolution obtained by thermoreflectance is more than an order of magnitude better than micro-thermocouples, and allows simultaneous temperature measurement of the entire SOA chip surface within a 1.7 mm × 1.3 mm field of view. Imaging of the entire SOA is desirable, since it enables full thermal and optical characterization along the length of the device, therefore the same magnification is used for all measurements reported here.

In order to calculate a change in power ($\Delta P_{el}, \Delta P_{rad}$) in the SOA from a measured change in surface temperature (ΔT_s), it is first necessary to determine the lumped material parameter c/L for the SOA. From (4), this calibration can be done using thermoreflectance by measuring the average change in temperature versus electrical pump power (ΔP_{el}). However, in practice, two additional subtleties must be accounted for: an offset

in the overall chip temperature and the noise level in the thermal measurements.

The chip offset temperature, which is uniform across the surface, reflects changes in the heat sink temperature that are represented by the factor γ described in Section III. Unlike γ, however, the slope of the chip offset temperature takes into account frequency dependent dynamics in the control of the thermoelectric cooler. To account for this offset, the average change in temperature is measured not only at the surface of the pumped SOA ridge but also away from the heat source at the gold contact of an adjacent unpumped device. Both the ridge and offset temperatures increase linearly with ΔP_{el}, and c/L is calculated as the difference between their two slopes [Fig. 2(c)]. For large PICs, such as the Alphion devices described here, the chip offset temperature is small and has negligible impact on the c/L parameter, and is therefore not shown in Fig. 2(c).

Shot noise from the illuminator (LED) and thermal noise in the CCD camera also contribute to an offset in the thermal image, and must be subtracted in order to get an accurate temperature reading. However, the noise level is independent of the surface temperature and can be determined from the illuminator intensity, camera exposure, and experiment run time [17].

For the results presented in this paper, the noise level is taken to be the temperature offset that is measured when the lock-in experiment is run without temperature modulation.For SOA 1, this thermoreflectance calibration technique gives a value of approximately 1.4 W/K.cm for c/L in (4). The same value of 1.4 W/K.cm for c/L is obtained using micro-thermocouples by measuring r, Z_T and $A_{\text{eff}} \cdot h$, employing the method used in [18]. This consistency between the two different measurements of c/L, which relates a measured change in SOA ridge temperature to a change in injected optical or electrical power, demonstrates the equivalence of thermoreflectance and micro-thermocouples for measuring changes in SOA surface temperature with power. In prior work, such micro-thermocouple temperature measurements have been demonstrated as an accurate means to measure the optical power distribution in an SOA [11]. Here, we report thermoreflectance as a non-invasive, high resolution alternative to micro-thermocouple measurements.

B. Thermal Imaging for Optical Characterization of SOAs and Inter-SOA Loss in PICs

Thermal imaging has also been used to optically characterize SOAs to determine fiber coupling loss and optical gain. Fig. 3(a) shows the thermal profile along the waveguide ridge, when SOA 1 is unbiased and acting as an absorber, for an input optical power of 51.4 mW coupled into the left facet of the PIC. The input optical signal is provided by an external distributed feedback (DFB) laser ($\lambda = 1550$ nm) that is directly modulated with a sine wave at $f = 15$ Hz. Heating of 240 mK from optical absorption at the unbiased SOA input can be clearly seen in the temperature profile of Fig. 3(a), with the exponential decay in the temperature being proportional to the absorbed optical power. From this, the total power absorbed by the unbiased SOA is calculated from (5) and the fiber coupling loss can be determined. Absorbed optical power was measured using both thermoreflectance and photocurrent (for photocurrent measurements the SOA is biased at -2 V and a conversion of 0.8 mW/mA is used) for a number of input optical powers, ranging from 5 mW to 26 mW, with both measurement techniques showing an average fiber coupling loss of 4.5 dB [Fig. 3(b)]. This value is consistent with coupling loss reported by Alphion, after taking into account loss due to free carrier absorption from doping in the passive input waveguide. From this absorption data, the precision of the thermoreflectance measurement can also be calculated, and is shown here to be within 1 mW of the expected value as measured by photocurrent.

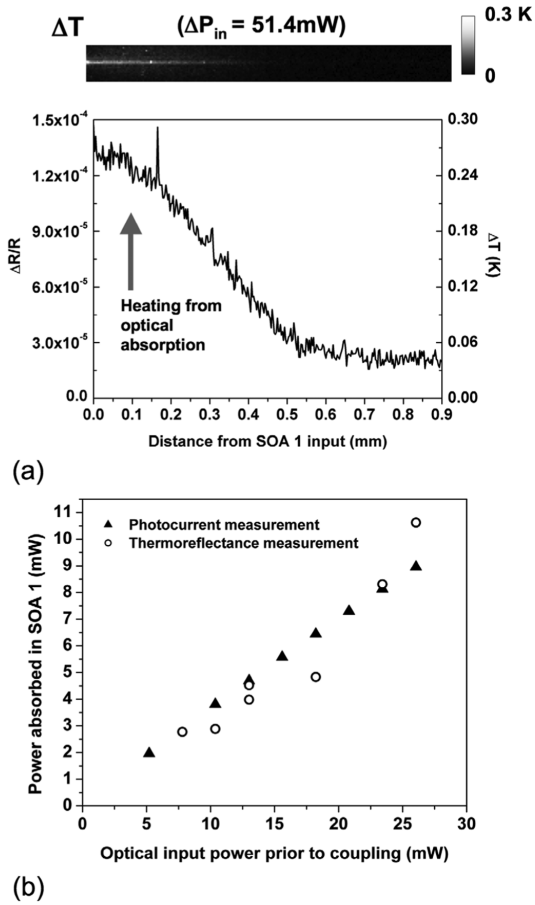

Fig. 3. Optical absorption measurements to determine fiber coupling loss in an unbiased SOA. (a) Thermal image (top) and temperature profile along SOA ridge for heating from optical absorption when the SOA is unbiased. (b) Thermoreflectance and photocurrent measurements of absorbed optical power in the SOA for different input optical powers, showing an average fiber coupling loss of 4.5 dB and a precision of 1 mW using thermoreflectance. For photocurrent measurements, the SOA is reverse-biased at -2 V, and a conversion factor of 0.8 mW/mA is used, assuming one electron–hole pair is generated per photon absorbed.

Fig. 4(a) shows the thermal profile along the waveguide ridge, with a fixed input optical signal of $\Delta P_{\text{in}} = 3$ mW, for an SOA bias current of 300 mA. Here, the input signal is amplified, and an exponential increase in radiative cooling from stimulated emission is observed up to the SOA output (right facet). Unlike the absorption measurement shown in Fig. 3(a), ΔT is proportional to heat *removed* from the ridge during amplification, so the thermal profile of Fig. 4(a) has an experimentally measured 180° phase change compared to the absorption profile of Fig. 3(a). Integrating the temperature profile gives the optical power added to the modulated input optical signal, which

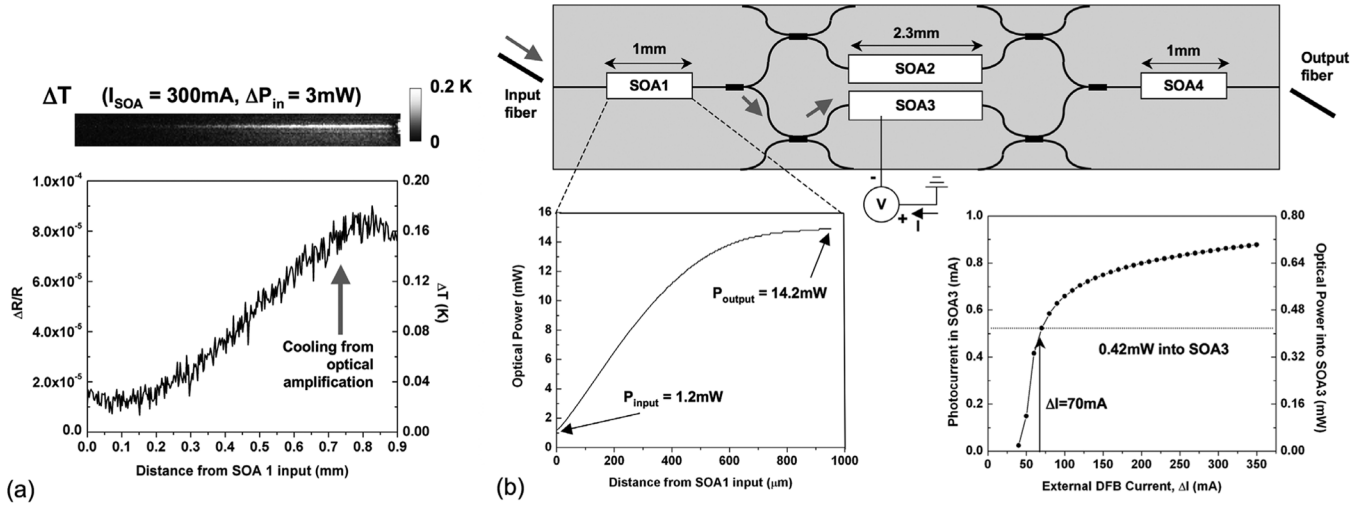

Fig. 4. (a) Thermal image (top) and temperature profile along SOA ridge for cooling from optical amplification when the SOA is biased at 300 mA (b) (top) Schematic of a part of an Alphion PIC used in the measurements. SOA1 and SOA4 are 1 mm and SOA2 and SOA3 are 2.3 mm in length. SOA1 and SOA4 are fiber coupled. (bottom left) Optical power in SOA1 calculated from the thermal image, for $\Delta P_{\rm inj} = 3$ mW into the input fiber, a fiber coupling loss of 4 dB, and an SOA1 bias current of 300 mA. (bottom right) Photocurrent measured in SOA3 as a function of external DFB laser bias current, for SOA1 biased at 300 mA and SOA3 biased at -2 V. The conversion factor of 0.8 mW/mA is used for the photocurrent measurements, assuming one electron–hole pair is generated per photon absorbed. The vertical arrow shows the DFB laser bias point used for the measurement.

can be used to calculate SOA gain. For the conditions used in Fig. 4(a), 1.2 mW of optical power is coupled into SOA 1, and is amplified to a power of 14.2 mW at the SOA output for an on-chip gain of 10.7 dB [Fig. 4(b), bottom left].

Since thermoreflectance allows measurement of the optical power at the input and output of each SOA, it is possible to characterize the total loss from couplers, s-bends, and other components between SOAs without the need for special test structures or destructive testing. Therefore, using the output power from SOA 1, thermoreflectance can be used to determine the total loss between the output of SOA 1 and the input to SOA 3, to account for the loss that the optical signal encounters as it is split and routed to one arm of the MZI structure.

In order to precisely measure power into the MZI SOAs, SOA3 is reverse biased at -2 V and its photocurrent is measured as a function of the external DFB laser bias current with SOA1 biased at 300 mA [Fig. 4(b), bottom right]. The DFB laser bias point used in the SOA1 thermal imaging measurement is shown with an arrow, indicating an optical power of 0.42 mW at the input to SOA3. From this, the total loss of the s-bends and splitters between SOA1 and SOA3 is calculated to be 15.3 dB.

This loss measurement, which is consistent with values reported by Alphion, cannot be determined by SOA photocurrent alone, and typically special test structures or electrodes are used to separately characterize splitter, waveguide, and s-bend losses. These measurements show that, by using a combination of thermoreflectance and photocurrent, inter-SOA loss can be measured on a functioning PIC, without the need for extra electrodes or test structures.

C. Fiber-Free Characterization of PICs Using ASE for Wafer Stage Testing

The final application of thermal imaging in this work involves development of a method for optically characterizing PICs at the wafer stage, prior to packaging and fiber-coupling. The results in Section IV-B relied on optical injection from an external source to the device via an input optical fiber. Here, we show that the usual external optical source can be omitted and instead, modulated amplified spontaneous emission (ASE) from a cascaded SOA on a chip can be used as the optical source to probe the radiative heating or cooling response (ΔT) of the other integrated elements on the chip. This method, which can be used at the wafer level before packaging and fiber-coupling of the PIC, is complementary to photocurrent measurements [10], [20]. In addition to being a diagnostic tool for catastrophic failure analysis of the PIC, it is also useful for extraction of material parameters such as modal gain, which cannot be obtained by conventional electronic methods [13].

The inset of Fig. 5(a) shows a schematic of a PIC, comprised of six cascaded SOAs. The performance of SOA1 on this PIC is characterized by electrically modulating the ASE from SOA2 ($I_0 = 190$ mA, $\Delta I = 100$ mA), without accessing any of the input or output optical fibers. This modulated ASE is injected into SOA1 via the integrated waveguide, eliminating the need for a modulated external optical source. SOA 1 is electrically biased at a dc level of 240 mA. As the input light injected from SOA 2 is amplified, optical cooling of about 40 mK along the length of SOA1 is observed as shown in Fig. 5(a).

In order to demonstrate this technique as a fiber-free diagnostic tool for catastrophic failure of a cascaded device, the temperature profile of a damaged SOA (SOA 1) on another chip with the same layout is measured using the same ASE-based technique, as shown in Fig. 5(b). The observed lack of optical cooling along the length of SOA 1 indicates that no amplification is occurring in this SOA, because either SOA1 or the waveguide interconnect is damaged. Independent fiber-coupled optical measurements confirmed that SOA1 is damaged, but no unusual behavior is detected from a standard IV curve [Fig. 5(b), inset].

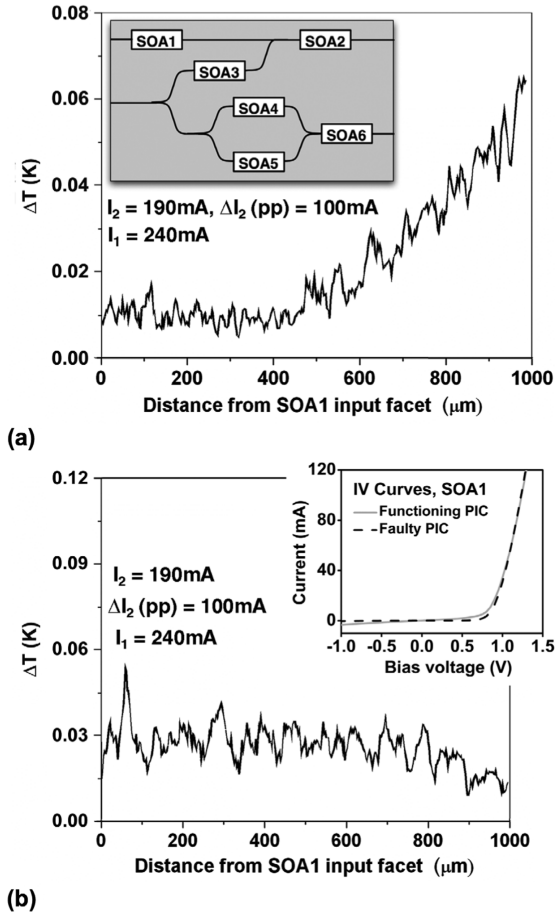

Fig. 5. (a) Schematic layout of the test PIC with six cascaded SOAs (inset) and temperature profile along the ridge of SOA1, using modulated ASE of SOA2. A cooling of about 40 mK is observed at the output facet. (b) Temperature profile along the ridge of SOA1 on a similar but faulty PIC, using ASE modulation of SOA2. No cooling is observed along the length of SOA1, indicating the catastrophic failure of this device or the waveguide interconnects. An IV curve of SOA1 on the faulty PIC (inset) shows no unusual behavior compared to the same SOA on a functioning PIC.

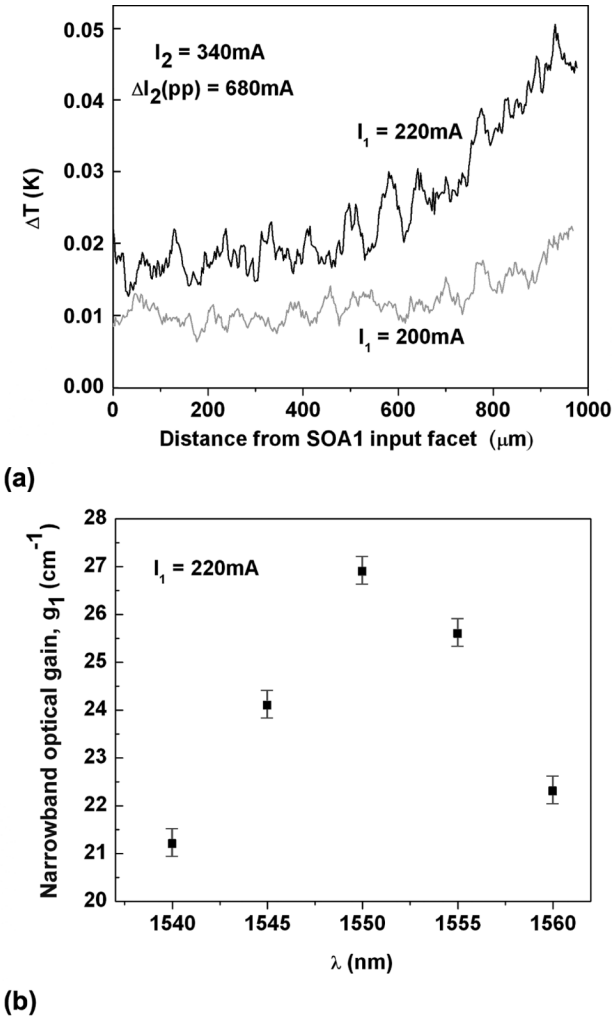

Fig. 6. (a) Temperature profile along the ridge of SOA1 in Fig. 4, biased at 200 mA and 220 mA, using modulated ASE of SOA2 as the light source. A cooling of about 30 mK is observed at the output facet at 220 mA. A broadband material gain of about 21 cm^{-1} is obtained from this profile at 220 mA. (b) Measured narrowband material gain of SOA1 at 220 mA, at different wavelengths of the injected light. The spectrally averaged gain from this plot is 24 cm^{-1} which is close to the broadband gain.

In addition to diagnosing catastrophic failures, this fiber-free technique can also quantify material parameters of cascaded devices, which is not achievable using conventional electronic testing. To demonstrate this, we use fiber-free thermoreflectance imaging to quantify the broadband gain per unit length of SOA 1 in the PIC shown in Fig. 4. The performance of SOA 1 is characterized, without accessing any of the input or output optical fibers, by electrically modulating the ASE from SOA 2. This modulated ASE is injected into SOA 1 via the integrated waveguides and splitters. SOA 1 is electrically biased at a fixed dc level and the bias current to SOA 2 is modulated by $\Delta I = \pm 340$ mA around a dc level of 340 mA. As the input ASE light injected from SOA 2 is amplified along the length of SOA 1, optical cooling due to the emitted photons is expected [11]. Fig. 6(a) shows the thermal profile of SOA 1 along the length of its waveguide ridge. When the SOA is biased near transparency ($I = 200$ mA), very little change in temperature can be seen along the length of the device. For a larger bias ($I = 220$ mA) gain is achieved, and a cooling of about 30 mK can be observed at the output facet.

The finite element energy balance model of (5) can be used once more to extract the material gain per unit length of SOA 1 from the temperature profiles of Fig. 6(a). From an exponential fit in the form of $\Delta P_{\text{out}}(x) = \Delta P_{\text{in}} e^{gx}$, where g is the modal gain of SOA 1 corresponding to the broadband ASE injection, values of $g = 17$ cm^{-1} and 21 cm^{-1} are extracted for $I_1 = 200$ mA and 220 mA, respectively.

For confirmation of this result, the single-wavelength, narrowband modal gain of SOA1 at 220 mA is also measured at five different wavelengths, ranging from 1540 nm to 1560 nm, by injecting an input signal from an external tunable laser. Using the same exponential fit for $\Delta P_{\text{out}}(x)$ in (5), the measured values for the narrowband gain are plotted as a function of wavelength in Fig. 6(b). From this data, a spectrally averaged modal gain value of $\langle g \rangle = 24$ cm^{-1} is obtained, which corresponds to a 10.4 dB increase in power for the 1-mm long SOA1. This is close to the broadband gain value of 21 cm^{-1} (9.1 dB/mm) extracted from the ASE experiment, with the 1.3 dB decrease in

measured gain for the ASE experiment likely due to the extra heat generated by electrical pumping of SOA2.

Hence, using the ASE of an on-chip SOA as the optical probe to analyze other cascaded devices on the chip is demonstrated to be a useful technique to extract the material parameters of integrated devices without requiring access to optical input and output fibers. This technique is potentially useful for testing of PICs at the wafer stage, prior to packaging and fiber-coupling.

V. Conclusion

In conclusion, we have demonstrated the use of a high resolution, large area, non-invasive thermoreflectance imaging technique for simultaneous thermal and optical characterization of SOA-based photonic integrated circuits under normal operating conditions. The thermal imaging technique enables detailed mapping of the optical power distribution along the length of an operating SOA, for measurement of optical input power, output power, and gain, without the need for extra electrodes or direct access to the optical signal.

In particular, we have shown the application of thermal imaging for precise temperature measurements, to quantify electrical heating in an SOA, and to determine the key optical characteristics of a photonic integrated circuit. Thermoreflectance was used to measure fiber-to-waveguide coupling loss, optical path loss between two SOAs (e.g., waveguide/splitting loss), and on-chip SOA gain without having to measure power in the fiber prior to coupling. Measurements were made using both external and integrated optical sources, and successfully shown to diagnose catastrophic failures and extract material gain. The ability to characterize and test the integrity of devices without the use of an external optical source makes this technique a valuable resource for wafer-scale testing, and provides a non-invasive means to screen devices prior to packaging.

The obtained information from thermal imaging of PICs would be valuable for improvements in chip thermal management, design of individual devices and PIC layout, and reduction of manufacturing costs.

Acknowledgment

The authors would like to thank P. Mayer, D. Lüerßen, G. Lakshminarayana, and B. Stefanov for their contributions and the Alphion Corporation for providing the devices.

References

[1] F. Ratovelomanana, N. Vodjdani, A. Enard, G. Glastre, D. Rondi, R. Blondeau, C. Joergensen, T. Durhuus, B. Mikkelsen, K. E. Stubkjaer, A. Jourdan, and G. Soulage, "An all-optical wavelength-converter with semiconductor optical amplifiers monolithically integrated in an assymetric passive Mach–Zehnder interferometer," *IEEE Photon. Technol. Lett.*, vol. 7, pp. 992–994, 1995.

[2] M. Settembre, F. Matera, V. Hagele, I. Gabitov, A. W. Mattheus, and S. K. Turitsyn, "Cascaded optical communication systems with in-line semiconductor optical amplifiers," *J. Lightw. Technol.*, vol. 15, pp. 962–967, 1997.

[3] K. E. Stubkjaer, "Semiconductor optical amplifier-based all-optical gates for high-speed optical processing," *IEEE J. Sel. Top. Quantum Electron.*, vol. 6, pp. 1428–1435, 2000.

[4] M. J. Connelly, *Semiconductor Optical Amplifiers*. Boston, MA: Kluwer Academic, 2002.

[5] C. Joergensen, S. L. Danielsen, K. E. Stubkjaer, M. Schilling, K. Daub, P. Doussiere, F. Pommerau, P. B. Hansen, H. N. Poulsen, A. Kloch, M. Vaa, B. Mikkelsen, E. Lach, G. Laube, W. Idler, and K. Wunstel, "All-optical wavelength conversion at bit-rates above 10 gb/s using semiconductor optical amplifiers," *IEEE J. Sel. Top. Quantum Electron.*, vol. 3, pp. 1168–1180, 1997.

[6] T. Durhuus, B. Mikkelsen, C. Joergensen, S. L. Danielsen, and K. E. Stubkjaer, "All-optical wavelength conversion by semiconductor optical amplifiers," *J. Lightw. Technol.*, vol. 14, pp. 942–954, 1996.

[7] J.-N. Fehr, M.-A. Dupertuis, T. P. Hessler, L. Kappei, D. Marti, P. E. Selbmann, B. Deveaud, J. L. Pleumeekers, J.-Y. Emery, and B. Dagens, "Direct observation of longitudinal spatial hole burning in semiconductor optical amplifiers with injection," *Appl. Phys. Lett.*, vol. 78, pp. 4079–4081, Jun. 2001.

[8] M. A. NewKirk, U. Koren, B. I. Miller, M. D. Chien, M. G. Young, T. L. Koch, G. Raybon, C. A. Burrus, B. Tell, and K. F. Brown-Goebler, "Three-section semiconductor optical amplifier for monitoring of optical gain," *IEEE Photon. Technol. Lett.*, vol. 4, pp. 1258–1260, Nov. 1992.

[9] K. L. Hall, E. P. Ippen, and G. Eisenstein, "Bias-lead monitoring of ultrafast nonlinearities in ingaasp diode laser amplifiers," *Appl. Phys. Lett.*, vol. 57, pp. 129–131, 1990.

[10] U. Koren, B. I. Miller, G. Raybon, M. Oron, M. G. Young, T. L. Koch, J. L. DeMiguel, M. Chien, B. Tell, K. Brown-Goebler, and C. A. Burrus, "Integration of 1.3 μm wavelength lasers and optical amplifiers," *Appl. Phys. Lett.*, vol. 57, pp. 1375–1377, Oct. 1990.

[11] J. A. Hudgings, K. P. Pipe, and R. J. Ram, "Thermal profiling for optical characterization of waveguide devices," *Appl. Phys. Lett.*, vol. 83, pp. 3882–3884, 2003.

[12] D. Lueerssen, R. J. Ram, A. Hohl-AbiChedid, E. Clausen, Jr., and J. A. Hudgings, "Thermal profiling: Locating the onset of gain saturation in semiconductor optical amplifiers," *Photon. Techol. Lett.*, vol. 16, pp. 1625–1627, 2004.

[13] M. Farzaneh, J. A. Hudgings, and R. J. Ram, "Fiber-free characterization of photonic integrated circuits by thermoreflectance microscopy," presented at the Conf. Laser and Electrooptics, Baltimore, MD, 2007.

[14] G. Lakshminarayana, J. Sarathy, B. Stefanov, R. Mu, T. Thai, and D. Lowe, "A new architecture for counterpropagation-based photonic regeneration and shaping," presented at the Optical Fiber Commun. Conf., Anaheim, CA, 2005.

[15] S. Dilhaire, S. Grauby, and W. Claeys, "Thermoreflectance calibration procedure on a laser diode: Application to catastrophic optical facet damage analysis," *IEEE Electron Device Lett.*, vol. 26, pp. 461–463, Jul. 2005.

[16] S. Grauby, B. C. Forget, S. Hole, and D. Fournier, "High resolution photothermal imaging of high frequency phenomena using a visible charge coupled device camera associated with a multichannel lock-in scheme," *Rev. Sci. Instrum.*, vol. 70, pp. 3603–3608, Sep. 1999.

[17] P. M. Mayer, D. Lueerssen, R. J. Ram, and J. A. Hudgings, "Theoretical and experimental investigation of the thermal resolution and dynamic range of CCD-based thermoreflectance imaging," *J. Opt. Soc. Am. A*, vol. 24, pp. 1156–1163, Apr. 2007.

[18] K. P. Pipe and R. J. Ram, "Comprehensive heat exchange model for a semiconductor laser diode," *IEEE Photon. Technol. Lett.*, vol. 15, pp. 504–506, Apr. 2003.

[19] M. Farzaneh, D. Lueerssen, and J. Hudgings, "Thermal profiling of photonic integrated circuits by thermoreflectance microscopy," presented at the Conf. Lasers and Electrooptics, 2006.

[20] N. K. Dutta, A. B. Piccirilli, M. S. Lin, and T. R. Halemane, "Monitoring the performance of a semiconductor optical amplifier," *Appl. Phys. Lett.*, vol. 57, pp. 659–660, Aug. 1990.

Joseph A. Summers (M'07) received the B.Sc. degree from Northwestern University, Evanston, IL, and the M.S. and Ph.D. degrees from the University of California, Santa Barbara, in 2000, 2004, and 2007, respectively, all in electrical engineering.

He is currently a Postdoctoral Researcher in the Physics Department at Mount Holyoke College, South Hadley, MA. His research interests include high-resolution thermal imaging of optoelectronics, and design and fabrication of photonic integrated circuits.

Maryam Farzaneh received the B.Sc. and M.Sc. degrees in physics from Sharif University of Technology, Tehran, Iran, in 1996 and 1998, respectively. She

received the Ph.D. degree in physics from Boston University, Boston, MA, in 2006.

She was a Postdoctoral Research Associate in the Department of Physics, Mount Holyoke College, South Hadley, MA, from 2005 to 2007. She is currently a visiting Assistant Professor at the Department of Physics and Astronomy, Denison University, Granville, OH. Her research interests include thermoreflectance microscopy and thermography techniques in photonic devices and integrated circuits.

Rajeev J. Ram (M'96–SM'07) received the Ph.D. degree in electrical engineering from the University of California, Santa Barbara, in 1997, and the B.S. degree in applied physics from Caltech in 1991.

He is Professor of electrical engineering and computer science at the Massachusetts Institute of Technology (MIT), Cambridge, MA. He serves as Director of the MIT Center for Integrated Photonic Systems and Associate Director of the Research Laboratory of Electronics. He leads the Physical Optics and Electronics Group which focuses on optoelectronic devices for applications in communications, biological sensing, and energy production.

Janice A. Hudgings (M'99–SM'06) received the B.S. degree in engineering and the B.A. degree in mathematics from Swarthmore College, PA, in 1991, and the M.Sc. degree in mathematics from Oxford University, Oxford, U.K., in 1994, where she studied as a Rhodes Scholar. She received the Ph.D. degree in electrical engineering from the University of California, Berkeley, in 1999.

She is currently an Associate Professor of physics at Mount Holyoke College, South Hadley, MA, as well as the co-founder and Vice President of Alenas Imaging, Inc. Her research interests include high resolution thermography of optoelectronic devices and advanced materials, optical feedback, and photonic devices including VCSELs and wavelength converters.

Dr. Hudgings won the Optical Society of America's Esther Hoffman Beller medal in 2004 and an NSF Career Award in 2002.